

Cluster-size dependence of electron capture and excitation cross sections in proton- Na_n collisions

F. Martín

Departamento de Química, C-9, Universidad Autónoma de Madrid, 28049 Madrid, Spain

M. F. Politis

GPS, Université de Paris VII, 2 place Jussieu, 75251 Paris, France

B. Zarour, P. A. Hervieux, J. Hanssen, and M. E. Madjet
LPMC, Institut de Physique, Technopôle 2000, 57078 Metz, France

(Received 1 June 1999)

We have evaluated electron capture and excitation cross sections for $\text{H}^+ + \text{Na}_n$ collisions ($n = 8, 20, 40, 92$) in the impact energy range 40–500 eV. The theoretical method includes the many-electron aspect of the problem and makes use of realistic cluster potentials obtained with density-functional theory and a spherical jellium model. Both electron capture and excitation cross sections increase monotonically with cluster size, but the rate of this increase is much more pronounced than expected from purely geometrical considerations. Also, capture cross sections are between one and two orders of magnitude larger than the geometrical cross sections. For the larger systems, our results differ from recent theoretical estimates obtained at higher impact energies. [S1050-2947(99)08611-4]

PACS number(s): 36.40.Sx, 34.70.+e

I. INTRODUCTION

Recent experimental works have shown that low energy collisions of highly charged ions with metal clusters are efficient ways to produce positively charged clusters [1,2]. An interesting application is the formation of clusters with critical charge-size ratios that may be difficult to produce using standard photoionization techniques. This has been spurred during this decade by the important progress in the production of mass-selected clusters with a well defined number of alkali-metal atoms [3]. Despite these experimental efforts, the basic mechanisms leading to electron capture are not yet well understood. This is due in part to the large number of active electrons, which may lead to multiple processes [4–6] that cannot be described in terms of a single electron picture. To better understand electron capture processes, recent theoretical attempts have mainly concentrated on collisions of metal clusters with *one-electron* atoms (mostly alkali metals) [7–9] or singly charged ions (mostly protons) [10–12]. In the first case, some experimental information is also available [13].

An important aspect of the problem is the cluster-size dependence of the capture cross sections (see, e.g., the experiments of Ref. [13]). Such a study has been performed theoretically by Børve and Hansen [10] for the case of $\text{H}^+ + \text{Na}_n$ collisions at 1–16 KeV impact energies from $n = 1$ to 75. Apart from statistical factors, these authors have used a single electron model in which the cluster potential is represented by a spherical box modified by a Coulomb tail. A fully microscopic description including all the active electrons of the problem as well as all nuclear degrees of freedom is only possible for small metal clusters (typically containing fewer than 10 atoms [8,9]). However, recent theoretical developments [11,12] have shown that, for medium-size closed-shell metal clusters, it is still possible to account for the many-electron aspect of the problem by freezing the cluster nuclear degrees of freedom during the

collision. A necessary condition for the validity of this approximation is that the collision time is much shorter than the vibrational period of the cluster ionic cores.

The simplest way to implement such an idea is using the spherical jellium model [14] to represent the cluster ionic background. This model leads to an accurate description of the shell structure and ionization potential of closed-shell metal clusters, and has been used by several authors in the context of ion(atom)-cluster collisions [4,7,15]. In Refs. [11,12] we have used this approximation to study electron capture and excitation for the $\text{H}^+ + \text{Na}_{20} \rightarrow \text{H} + \text{Na}_{20}^+$ reaction. Here, we extend the study to Na_8 , Na_{40} , and Na_{92} closed-shell clusters and analyze the behavior of neutralization and excitation cross sections as functions of cluster size. The theoretical method is inspired by the molecular approach of ion-atom collisions and, therefore, it is aimed at investigating collisions at impact velocities smaller than that of cluster electrons (see below). For this reason, in this work we have restricted ourselves to impact energies smaller than 0.5 KeV.

The paper is organized as follows. In Sec. II, we briefly outline the theoretical method. We present in Sec. III the calculated cross sections and the potential energy curves that are relevant for the collision study. We end the paper with some conclusions in Sec. IV. Atomic units are used throughout unless otherwise stated.

II. THEORETICAL METHOD

The electrons are described as moving in both the effective potential representing the cluster and the projectile potential (this is also the case for the *molecular* method in ion-atom collisions). Closed-shell Na clusters, such as those considered in this work, are accurately described by the spherical jellium model [14], which consists in replacing the real ionic core potential by a constant positive background of radius R_C . In this context, we apply the Kohn-Sham formulation of density-functional theory and describe the cluster

electron density in terms of single-particle orbitals. The corresponding one-electron potentials, V_C , have been obtained using a local-density approximation with exchange, correlation, and a self-interaction correction (see Ref. [11] for details). The latter correction ensures the correct asymptotic behavior $-1/r$ of the potential, which is crucial in the present study because capture and excitation processes occur mainly at large distances. An important consequence of the quasiseparability of the cluster Hamiltonian is that the total N -electron Hamiltonian $\hat{\mathcal{H}}$ can be written as a sum of one-electron effective Hamiltonians, $\hat{\mathcal{H}} = \sum_{i=1}^N \hat{h}(i)$, with

$$\hat{h} = -\frac{1}{2} \nabla^2 + V_p(|\mathbf{r} - \mathbf{R}|) + V_C(\mathbf{r}), \quad (1)$$

where V_p is the proton Coulomb potential, $V_p = -1/|\mathbf{r} - \mathbf{R}|$, and V_C is the cluster potential. Notice that the origin of electronic coordinates has been placed on the cluster center; \mathbf{R} is the proton position vector. Thus, the N -body dynamical treatment reduces to the study of N single-particle problems. This is equivalent to the independent electron model (IEM) of atomic collisions.

We treat the collision in the framework of the impact parameter method, i.e., the projectile follows a straight line trajectory whereas the electrons are described quantum mechanically. Assuming that each electron i is initially in a $\phi_i(\mathbf{r})$ spin orbital of energy ϵ_i , then one has to solve a set of N time-dependent Schrödinger equations

$$\hat{h} \psi_i(\mathbf{r}, t) = i \frac{d}{dt} \psi_i(\mathbf{r}, t), \quad i = 1, \dots, N, \quad (2)$$

where each $\psi_i(\mathbf{r}, t)$ is subject to the initial condition

$$\lim_{t \rightarrow t_0} \psi_i(\mathbf{r}, t) = \phi_i(\mathbf{r}) \exp[-i \epsilon_i t_0]. \quad (3)$$

The transition probability to a specific final configuration $(f_1, \dots, f_N) = \|\phi_{f_1} \cdots \phi_{f_N}\|$ is given by the $(N \times N)$ determinant [16]:

$$P_{f_1, \dots, f_N} = \det(\gamma_{nn'}); \quad n, n' = 1, \dots, N, \quad (4)$$

where $\gamma_{nn'}$ is the one-particle density matrix, $\gamma_{nn'} = \langle f_n | \hat{\rho} | f_{n'} \rangle$, and $\hat{\rho}$ is the density operator which accounts for the time evolution of the spin orbitals. Since all processes leading to the same final state of the projectile contribute to the measured cross section, one has to evaluate *inclusive* cross sections [16]. The inclusive probability P_{f_1, \dots, f_q} of finding q of the N electrons in the subconfiguration (f_1, \dots, f_q) while the remaining $N - q$ ones occupy any other states is given by an ordered sum over all exclusive probabilities, which include that subconfiguration. This probability is given by the $(q \times q)$ determinant [16]

$$P_{f_1, \dots, f_q} = \det(\gamma_{nn'}); \quad n, n' = 1, \dots, q; \quad q < N. \quad (5)$$

The inclusive probability of finding q occupancies and $L - q$ holes, $P_{f_1, \dots, f_q}^{f_{q+1}, \dots, f_L}$, can be written in terms of probabilities (5) related only to occupancies (see Ref. [16]). As shown in [11], the latter probabilities can be used to evaluate the energy deposit after the collision. Since we are dealing with

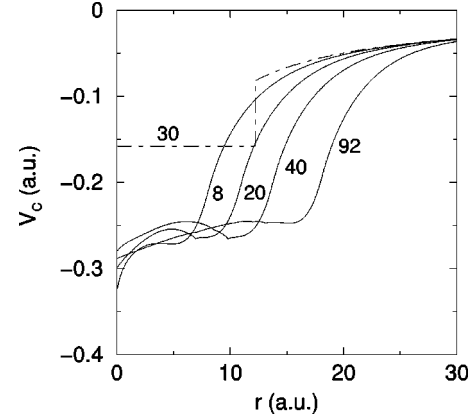


FIG. 1. Calculated cluster potentials V_C for Na_8 , Na_{20} , Na_{40} , and Na_{92} using the theory described in Sec. II. The chain line shows the potential used by Børve and Hansen [10] for Na_{30} .

neutral clusters and the impact energy is rather low, the energy deposit is not large enough to induce significant cluster fragmentation (Ref. [11] shows in fact that, for N_{20} , only a monomer may be evaporated, but with an extremely long lifetime). For this reason, we have not computed the energy deposits in the present work.

III. CALCULATIONS AND RESULTS

The calculated one-electron potentials for Na_8 , Na_{20} , Na_{40} , and Na_{92} are shown in Fig. 1. We have included in the same figure the potential used by Børve and Hansen for Na_{30} . As can be seen in the figure, the calculated V_C potentials do not exhibit a steplike behavior around $r = R_C$. More interestingly, the classical Coulomb behavior is only observed at very large values of r . We will see below that this has important consequences on the values of the calculated cross sections. The calculated ionization potentials are 4.7, 4.1, 3.8, and 3.8 eV, respectively, to be compared with the experimental values 4.2, 3.8, 3.6, and 3.5 eV [3].

Now, in order to solve the time-dependent Schrödinger equations associated with the single-particle Hamiltonian in Eq. (1), one has to expand the one-electron wave functions in a basis of Born-Oppenheimer (BO) *molecular* states $\{\chi_k(\mathbf{r}, \mathbf{R})\}$. These states have been obtained by diagonalizing \hat{h} in a two-center *atomic* basis built from spherical Gaussian-type orbitals (GTO) with angular momentum up to $l = 6$. In Fig. 2 we show the BO potential energy curves for the σ states of the $(\text{Na}_8\text{-H})^+$, $(\text{Na}_{20}\text{-H})^+$, $(\text{Na}_{40}\text{-H})^+$, and $(\text{Na}_{92}\text{-H})^+$ *quasimolecules*. The occupied orbitals are, respectively, $1s$ and $1p$ for Na_8 , $1s$, $1p$, $1d$, and $2s$ for Na_{20} , $1s$, $1p$, $1d$, $2s$, $1f$, and $2p$ for Na_{40} , and $1s$, $1p$, $1d$, $2s$, $1f$, $2p$, $1g$, $2d$, $3s$, and $1h$ for Na_{92} (for simplicity, we use the “separate atom” notation to refer to molecular orbitals). The highest occupied molecular orbital (HOMO) is, respectively, $1p$, $2s$, $2p$, and $1h$. Asymptotically occupied cluster orbitals mainly interact with the $n = 2$ orbitals of H. The latter are in fact Stark hybrids produced by the cluster electric field. It can be seen in the four cases that the energy curves associated with the HOMO present avoided crossings with the lowest Stark hybrid. The corresponding radial couplings have been evaluated as in Ref. [11] and present sharp maxima at around $R \approx 16, 20, 25,$

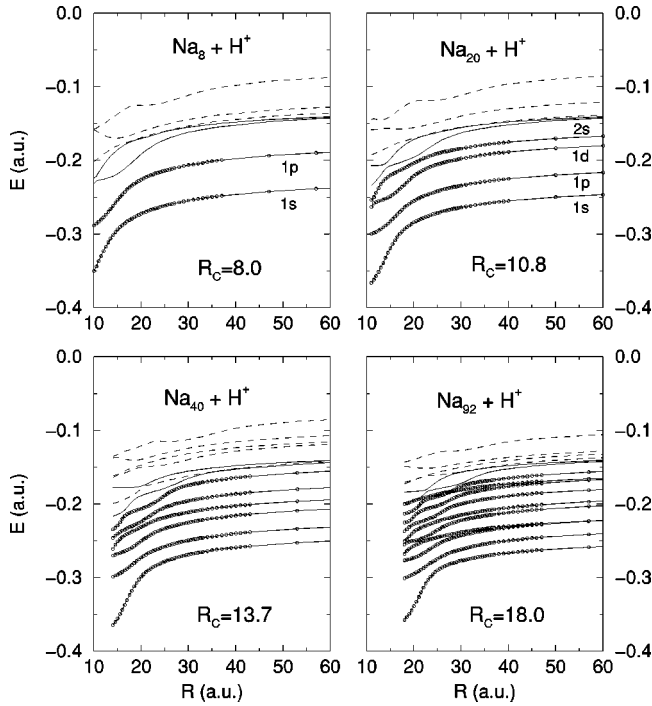


FIG. 2. Potential energy curves for the σ adiabatic states of the $(\text{Na}_n\text{-H})^+$ systems. Full lines: H-correlated states (capture channels); full lines with circles: occupied cluster states; dashed lines: empty cluster states. For the sake of clarity we have not included the labels of the occupied cluster orbitals in Na_{40} and Na_{92} . These labels are given in the text. Notice that, in the case of $\text{Na}_{40} + \text{H}^+$, the lowest unoccupied cluster channel exhibits a sharp avoided crossing with the dominant capture channel at $R \approx 35$ a.u. Thus, from the point of view of the collision dynamics, the dashed and continuum lines should be better exchanged beyond that value of R . However, for the sake of consistency we have preferred to use an adiabatic notation in all cases.

and 30 a.u., respectively. As radial couplings between π states are only important at smaller R , they do not play an important role in the collision dynamics. Thus, we have limited the expansion of ψ_i to *molecular* states of σ symmetry. In all cases we have included the two states dissociating into $\text{H}(n=2)$ (the Stark hybrids $\xi_{1,\text{H}}$ and $\xi_{2,\text{H}}$) and all the states dissociating into occupied cluster orbitals. In addition, we have included several states dissociating into unoccupied cluster orbitals, namely $1d$, $2s$, $2p$, $1f$, $3s$, and $2d$ for Na_8 , $1f$ and $2p$ for Na_{20} , $1g$, $2d$, $3s$, $1h$, $3p$, $1i$, $4s$, and $3d$ for Na_{40} , and $2f$, $3p$, $1i$, $2g$, $3f$, $4s$, and $2h$ for Na_{92} . This amounts to 10, 8, 16, and 19 states, respectively. These minimal sets of molecular states have allowed us to describe the capture reactions as well as cluster excitations.

We have evaluated the inclusive probabilities $P_{\xi_{1,\text{H}}}$ and $P_{\xi_{2,\text{H}}}$. As capture of more than one electron is very unlikely (it leads at most to the formation of H^- , which is a weakly bound anion), $P_{\xi_{1,\text{H}}}$ and $P_{\xi_{2,\text{H}}}$ can be interpreted as probabilities of finding *one* electron in the projectile. However, the solution of the one-electron time-dependent equations does not guarantee that the q -electron inclusive capture probabilities are negligible (as they should be physically). In that case, one would overestimate the neutralization probability

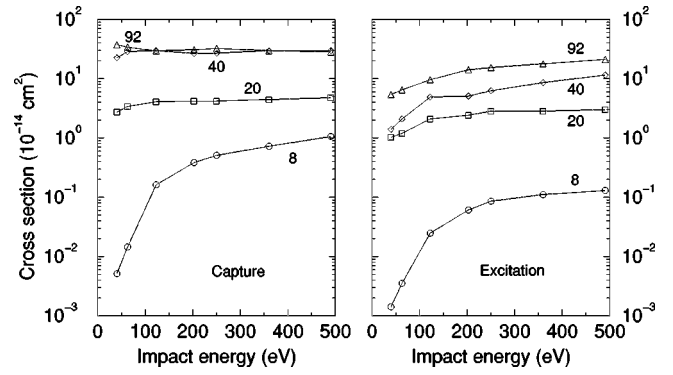


FIG. 3. Electron capture and excitation cross sections for $\text{H}^+ + \text{Na}_n$ collisions. Numbers indicate values of n .

by overcounting the artificial many-electron capture probabilities. To check this particular point we have evaluated the two-electron capture probability $P_{\xi_{1,\text{H}}\xi_{2,\text{H}}}$ for the $\text{Na}_{40} + \text{H}^+$ collision. For all impact energies investigated here, the corresponding cross sections are less than 1% of the total neutralization cross sections reported below. This supports the interpretation that $P_{\xi_{1,\text{H}}}$ and $P_{\xi_{2,\text{H}}}$ mainly represent one-electron capture probabilities.

The probabilities $P_{\xi_{1,\text{H}}}$ and $P_{\xi_{2,\text{H}}}$ do not correspond to pure single capture reactions, but to a sum of reactions whose common feature is to yield neutral H atoms. They include, in particular, single capture + excitation processes. The importance of this many-particle process has been discussed in detail in Ref. [11] for the case of the $\text{Na}_{20} + \text{H}^+$ collision. Similar conclusions have been obtained in this work for the other three systems, namely that capture excitation has an increasing non-negligible contribution to the capture cross section when the collision velocity increases.

The total *capture* (i.e., *neutralization*) probability is defined as $\hat{P}_{n=2,\text{H}} = 2(P_{\xi_{1,\text{H}}} + P_{\xi_{2,\text{H}}})$. Addition of $P_{\xi_{1,\text{H}}}$ and $P_{\xi_{2,\text{H}}}$ does not lead to overcounting because the only configurations included in both inclusive probabilities are those with two or more electrons on the projectile, which, as discussed above, barely contribute to the total probability. The factor of 2 appears because the captured electron can have either α or β spin components. In all cases we have found that the largest contribution to the total capture probabilities comes from the region of large impact parameters ($b \sim 20\text{--}30$ a.u. for Na_{20}). Similarly, we define the total *excitation* probabilities $\hat{P}_{\text{ex}} = \sum_i [2P_i - (P_i)^2]$, where i stands for cluster orbitals that are empty at the beginning of the collision. The $(P_i)^2$ term corrects for overcounting of double excitations to the same orbital i . Similar terms should be included in order to correct for overcounting of double excitations to different orbitals, however they have been neglected because these terms are expected to be small.

The neutralization and excitation cross sections are shown in Fig. 3 as functions of impact energy. In all cases, the total excitation cross sections are smaller than the neutralization cross sections. We can observe that the latter increase with impact energy for the smaller systems, Na_8 and Na_{20} , and are practically flat for the larger ones, Na_{40} and Na_{92} . In contrast, excitation cross sections are increasing functions of impact energy in all cases. It can be also observed that both

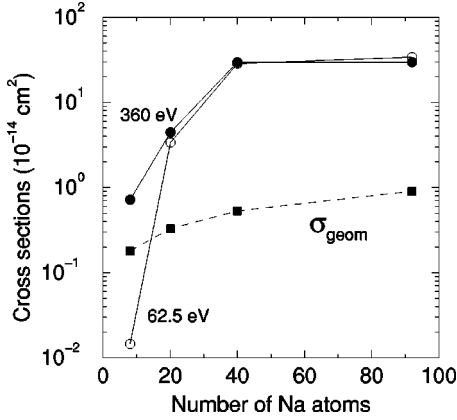


FIG. 4. Capture cross sections as functions of the number of cluster sodium atoms for two different values of the impact energy. The dashed line is the geometrical cross section obtained with the formula πR_C^2 .

capture and excitation cross sections increase with cluster size; in contrast, the rate of this increase decreases with size. This is more clearly shown in Fig. 4, where we have plotted the calculated capture cross section as functions of cluster size for impact energies of 62.5 and 360 eV. In the latter figure we have included for comparison the value of the corresponding geometrical cross sections, $\sigma_{\text{geom}} = \pi R_C^2$, using the values of R_C given in Fig. 2. We conclude from this comparison that the value of the neutralization cross section is not only much larger than that of the geometrical cross section, but also that the rate of increase is not due to purely geometrical effects. The observed behavior is related to the position of the avoided crossings between capture channels and the states dissociating into occupied orbitals of the cluster.

Finally, we have compared in Fig. 5 our results for the neutralization cross sections with those of Børve and Hansen [10]. Although we have explored a different region of impact energies, several conclusions can be extracted from this comparison. The first one is that our results for Na_8 and Na_{20} match reasonably well those of Ref. [10]. Hence, the maximum of the neutralization cross sections seems to be around 1 KeV, which corresponds to an impact velocity of 0.2 a.u., well below the Fermi velocity, v_F , of the cluster electrons. This result confirms that inner cluster electrons, with $v < v_F$, play a significant role in the collision dynamics (this point has been already shown in [11] for the case of Na_{20}). It is also a consequence of the important role of excitation and many-electron processes. For Na_{40} and Na_{92} , our results and those of Ref. [10] differ by an order of magnitude. There are several possible explanations for this discrepancy. First, many-electron processes not included in [10] become increasingly important when the cluster size increases, thus leading to larger cross sections. Second, in contrast with Ref. [10] where only $l=0$ orbitals were included, the dominant capture channels do not involve $l=0$ orbitals for the larger clusters. Furthermore, the relative number of $l=0$ electrons reduces dramatically for the latter clusters (see Fig. 1 and the discussion above). Third, the steplike behavior of the cluster potential used in [10] becomes a much poorer representation of the real potential because it is not able to reproduce the increasing electron spill out (see Fig. 1). Again, the latter

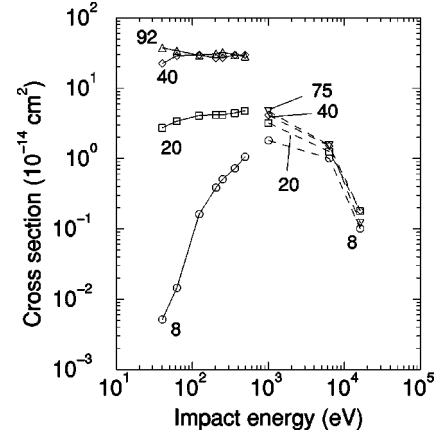


FIG. 5. Capture cross sections as functions of impact energy for $\text{H}^+ + \text{Na}_n$ collisions. Numbers indicate values of n . Full lines: present results. Dashed lines: results from Børve and Hansen [10]. The latter cross sections have been obtained from interpolation of the calculated values in Ref. [10]. The Na_{92} results have not been interpolated because the largest value of n reported in [10] is $n = 75$.

effect goes in the direction of increasing the values of the calculated cross sections. In any case, additional theoretical calculations and experiments would be desirable in order to better understand the origin of the discrepancy.

IV. CONCLUSION

In this paper we have investigated the cluster-size dependence of electron capture and excitation cross sections for collisions of protons with closed-shell sodium clusters in the impact energy range 40–500 eV. The theoretical method [11] treats the collision semiclassically and makes use of the independent electron model. The clusters are described in the jellium approximation using a Kohn-Sham formalism with a local-density approximation which includes exchange, correlation, and a self-interaction correction. The theory allows us to account for many-electron processes such as multiple excitations, simultaneous capture, and excitation, etc., which cannot be neglected in these kinds of collisions. We have found that both electron capture and excitation cross sections increase monotonically with cluster size, but the rate of this increase is much more pronounced than expected from purely geometrical considerations. Also, capture cross sections are much larger than the geometrical cross sections. Although these conclusions are in qualitative agreement with those previously reported by Børve and Hansen [10], we have found significant discrepancies for the larger systems investigated here. We hope the present results will stimulate experimental work in order to clarify the situation.

ACKNOWLEDGMENTS

The authors gratefully acknowledge Dr. I. Sánchez for his invaluable computational assistance. This work has been partially supported by the DGICYT project No. PB96-0056. We would like to thank the CNUSC (Center National Universitaire Sud de Calcul) and the CCCFC (Centro de Computación Científica de la Facultad de Ciencias de la UAM) for their generous allocation of computer time.

- [1] F. Chandezon, C. Guet, B. A. Huber, D. Jalabert, M. Maurel, E. Monnard, C. Ristori, and J. C. Rocco, *Phys. Rev. Lett.* **74**, 3784 (1995).
- [2] C. Guet, X. Biquard, P. Blaise, S. A. Blundell, M. Gross, B. A. Huber, D. Jalabert, M. Maurel, L. Plagne, and J. C. Rocco, *Z. Phys. D* **40**, 317 (1997).
- [3] W. A. de Heer, *Rev. Mod. Phys.* **65**, 611 (1993).
- [4] P. G. Reinhard, E. Suraud, and C. A. Ullrich, *Eur. Phys. J. D* **1**, 303 (1998).
- [5] A. Domsps, P.-G. Reinhard, and E. Suraud, *Phys. Rev. Lett.* **80**, 5520 (1998).
- [6] K. Yabana, T. Tazawa, Y. Abe, and P. Božek, *Phys. Rev. A* **57**, R3165 (1998).
- [7] M. Guissani and V. Sidis, *J. Chem. Phys.* **102**, 1288 (1995); *Z. Phys. D* **40**, 221 (1997).
- [8] U. Saalman and R. Schmidt, *Phys. Rev. Lett.* **80**, 3213 (1998).
- [9] O. Knospe, J. Jellinek, U. Saalman, and R. Schmidt, *Eur. Phys. J. D* **5**, 1 (1999).
- [10] K. J. Børve and J. P. Hansen, *Z. Phys. D* **25**, 247 (1993).
- [11] M. F. Politis, P. A. Hervieux, J. Hanssen, M. E. Madjet, and F. Martín, *Phys. Rev. A* **58**, 367 (1998).
- [12] F. Martín, P. A. Hervieux, J. Hanssen, M. E. Madjet, and M. F. Politis, *Phys. Rev. B* **58**, 6752 (1998).
- [13] C. Bréchnignac, Ph. Cahuzac, J. Leygnier, R. Pfaum, and J. Weiner, *Phys. Rev. Lett.* **61**, 314 (1988).
- [14] M. Brack, *Rev. Mod. Phys.* **65**, 677 (1993).
- [15] M. Gross and C. Guet, *Z. Phys. D* **33**, 289 (1995).
- [16] H.J. Lüdde and R.M. Dreizler, *J. Phys. B* **18**, 107 (1985).